



Support Vector Machine to Predict the Pile Settlement using Novel Optimization Algorithm

Qingyun Ge · Caimei Li · Fulian Yang

Received: 15 January 2023 / Accepted: 11 May 2023 / Published online: 22 June 2023
© The Author(s), under exclusive licence to Springer Nature Switzerland AG 2023

Abstract Project Immunization, like piled construction, requires considerations that make them safe during the period of operation. Pile Settlement (PS), a vital issue in projects, has attracted many regards to avoid failure before commencing employing constructions. Several factors in appraising the pile movement can assist in understanding the future of the project in the loading stage. Many intelligent strategies to mathematically compute the pile motion are employed to simulate the PS. The present study aims to use Support vector regression (SVR) to predict the settlement of piles. In addition, to improve the accuracy of the related model, two meta-heuristic algorithms have been used, including the Arithmetic Optimization Algorithm (AOA) and Grasshopper Optimization Algorithm (GOA), a hybrid format in the framework of SVR-AOA and SVR-GOA. Kuala Lumpur transportation network was chosen to investigate the pile motion according to the ground properties' condition with SVR-AOA and SVR-GOA developed frameworks. For the evaluation of each model's performance, five indices were employed. That, the values of *RMSEs* for SVR-AOA and SVR-GOA were obtained at 0.550 and 0.592, respectively, and *MAE*

exhibited the values of 0.525 and 0.561 alternatively. The R-value for the SVR-AOA showed a desirable magnitude of 0.994, which is 0.10% higher than the SVR-GOA. Also, *OBJ*, including *R*, *RMSE*, and *MAE*, for SVR-GOA and SVR-AOA were computed at 0.541 and 0.586 mm, respectively. Models' results have had a similar performance to estimating the PS rate.

Keywords Pile settlement · Support vector regression · Grasshopper optimization algorithm · Arithmetic optimization algorithm · RMSE

1 Introduction

Various studies expect the reaction of piles to the implemented axial load as discussed through the lectures with the aid of using relevant studies (Poulos 1989; Randolph 2003). The present knowledge of how piles reply beneath the load has improved many strategies researchers may utilize to estimate pile movement. Referred strategies were mentioned during the period by using many key researchers within the field, most notably by research (Stewart et al. 1994; Poulos 2006). These strategies vary from either easy-calculation methods via empirical and analytical strategies or finite element and finite difference numerical solutions. It is not always unusual while designing the basis for the pile to be based in a higher layer beneath the soil intensity accompanied by a

Q. Ge · F. Yang
West Anhui University, Lu'an 237012, Anhui, China

C. Li (✉)
Gates Winhere Automobile Water Pump Products(Yantai)
Co.LTD, Yantai 712000, Shandong, China
e-mail: ml1101@gates.com

much less compressible layer (Mishra et al. 2019; Kumar and Samui 2020).

This has been broadly acceptable with compressive sheets under the pile, which could significantly increase pile settlement, presenting a clear design challenge and risk. According to limited analysis, one research (Harry Poulos, 2017) proposes the incremental potential for subsidence due to the underlying layer, which can be significantly relevant to the geometry of the pile, soil, and its physical features. A study on this typical issue seems limited, and manual computational methods that looked analytical often seem unable to be considered for the existing distinct soil layers (Saggu 2022; Ma and Peng 2023).

Moreover, another research presented a way of analyzing the movement feasibility in a pile and introducing a theoretical function to study the coefficient of the pressure of the ground (Zhang et al. 2018a; b). The reference articles mainly evaluate pile motion, but none can be used directly without a ground reflection model. Further, solutions renowned as Artificial Neural Networks (ANN) and machine learning with proper ramifications through many types of research, Shanbeh et al. (Shanbeh et al. 2012), Che et al. (Che et al. 2003), Lee and Lee (Lee and Lee 1996), Liu et al. (Liu et al. 1997), and Hanna et al. (Hanna et al. 2004) used ways to predict some of the complex pile load problems. Present methods check parameters of pile settlement as well as pile friction and load capacity. Several studies have chosen the training data to complement and establish the predictive models to test the bearing capacity of piles and the motion. The data collection for the training set should be selected regarding the dynamic series in field investigations to provide modeling with a wide range of training data for an acceptable simulating process. A study (Goh 1996) that operated ANN attempted to form results on settlement characteristics of piles set up in rock. That data set related to the training stage was given through reports on actual piles in the field.

Regression techniques have been operated broadly, such as adaptive regression of multivariate splines, regression of Gaussian trend, and machine regression of minimax probability (Teodorescu and Sherwood 2008; Pal and Deswal 2010; Zhang and Goh 2013; Samui 2019; Benemaran and Esmaeili-Falak 2020; Momeni et al. 2020; Le and Le 2021). Strategies for some geotechnical problems are used via gene expression programming (GEP) (Teodorescu and Sherwood

2008; Alkroosh and Nikraz 2011; Mollahasani et al. 2011; Ozbek et al. 2013; Dindarloo 2015; Masoumi et al. 2020). Moodi et al. (2022) utilized MLP, RBFNN, and SVR models to estimate the compressive strength of concrete columns, and the correlation rates were calculated at 0.971, 0.973, and 0.901, respectively (Moodi et al. 2022). Chen et al. (2022) used 324 data sets with five independent input variables: water, cement, fine aggregate, coarse aggregate, and superplasticizer, to model the compressive strength with the conventional support vector regression (SVR) model. The results showed that SVR's prediction accuracy and reliability were $R^2=0.973$, $RMSE=1.595$, $MAE=0.312$, and $MAPE=2.469$ (Chen et al. 2022). This technique to find a way for the axial capacity of the pile has been examined in many studies (Alkroosh and Nikraz 2011). A novel formulation based on GEP was developed (Mollahasani et al. 2011). Another study was handled using three algorithms containing a support vector machine, multilayer perceptron, and GEP to predict the UCS of rock (Dindarloo 2015). The capability of the support vector machine to simulate the motion of a stratified sedimentary rock mass is clearly acceptable (Alemdag et al. 2016).

The support vector machine method has proposed more accurate and dependable calculation results (Gao and Han 2020; Ma et al. 2021; Acosta et al. 2021, 2023). Also, one study used this technique to evaluate the bearing capacity of piles (Teh et al. 1997). The data inputs contain soil characteristics, footing size, and reinforcement specimens from empirical or in-situ data measured (Soleimanbeigi and Hataf 2006). Regarding primary literature, the parameters comprising UCS of rock, the ratio of pile length to its cross-section diameter, loading masses, and ratio relevant to the depth of the pile length beneath the soil to rock, and N_{SPT} to appraise the displacement of piles (Shahin et al. 2002).

This article aims to better understand the problem of pile settlement socketed in rock using the support vector regression (SVR) technique to design the practical model of pile movement. With this respect, this paper has attempted to join, promote, and investigate a coupled model as SVR machine learning with optimization algorithms. In light of referred purpose, two novel optimization algorithms, Arithmetic Optimization (AOA) and Grasshopper Optimization Algorithm (GOA), were operated by SVR to enhance modeling

accuracy by finding optimum magnitudes of coefficients related to the machine learning process. The study novelties use novel algorithms to estimate the displacement of pillars socketed to rock with mentioned optimizers. The collection of experimental data to analyze pile motion and soil attributes was obtained from the Malaysia Transport Project in the Klang Valley Rapid Network (KVMRT) megacity of Kuala Lumpur.

The optimizers mentioned above, joined with the Support Vector Regressions (SVR), are productively examined for many complex issues because of their unique attributes, like being smart and straightforward. Both well-known techniques in the academic world have attracted much attention in the form of machine learning strategies used for many targets like biology, energy transformation analysis, and image processing (Alilou and Yaghmaee 2015; Bendu et al. 2016; Zendejboudi and Tatar 2017). The frameworks proposed as SVR-AOA and SVR-GOA provide the data gathered via penetrating the test and further static loading of on-ground indexes measured. Therefore, the pile loads, the parameters of the column length to the diameter ratio, the UCS parameter of rock, the length of the pillar beneath the soil to that rock ratio, as well as the N_{SPT} parameters were chosen to investigate the pile settlement in KVMRT project (Shahin et al. 2002). Several studies have examined the use of SVR in various engineering fields, such as predicting precipitation rates by combining machine learning techniques and algorithms for optimization (Wu et al. 2015; Xu et al. 2016). That sought to compute the optimal number of neurons in the so-called hidden layer within the process.

The variables required for figuring out the pile movement are specialized as five parameters, including pile length to its crossed diameter, the length under the soil to that of under the rock sheets ratio, bearing capacity as being ultimate, the strength of uniaxial compressive, standard penetration test, and pile subsidence as output and models' target. The main objective of the present research is to present a new way of coupling models with optimizers to estimate the optimum rate of model parameters for SVR. The present article has attempted to model the PS of pile samples by reproducing subsidence rates coupling with novel AOA and GOA optimization algorithms. Checking the dependability of the proposed model's demands using the wide range of indexes for

this research, R, MAE, OBJ, and RMSE were calculated to evaluate the modeling process. (Fig. 1).

2 Methodology

2.1 Preparing Primitive Dataset

Kuala Lumpur's most helpful transportation project to reduce traffic jams in Malaysia, called the Klang Valley Rapid Transit System (KVMRT), was the study area of the present research. Attention to the case study showed that thousands of bored piles were needed to support the transport stations in KVMRT. Same picture.1, presents the situation of Malaysia. Several stakes are driven on rocks, namely granite, phyllite, sandstone, and limestone.

Profiles of 96 granite-based piles were reviewed in this study. Within the region, the San Trias granite type was recorded. Subsurface information and materials were performed at the pile locations to verify common geological features. Based on the results, the structures of the underground subsoil are made up of residual rocks. Over the data collected, the depth of the bedrock ranges from 70 cm to more than 1400 m underground. With this respect, the sampling process among piles in the study area and relevant information and drilling log is described as follows:

- Values of UCS upon the ISRM were recorded at 25 MPa to 68 MPa, respectively, for lowest and highest (Hatheway 2009).
- Rock bulks were registered as moderately weathered to largely weathered.
- Between 7.5 to 27 m in the region at ground depth level, subsoil materials were recorded with N_{SPT} An index higher than 50 blows per 300 mm.
- 16.5 MPa was considered highly weathered soil based on the bore log data down to the deep underground. Hard sandy mud, including a minimum and maximum N_{SPT} Index of 4 and 167 blows per 300 mm, respectively, composed the predominant soil type.

The first stage in building a predictive model is organizing the best-fit data set with efficient state parameters. Identifying the important factors affecting model output is vital. The tests above were done using a tool of pile analyzing developed via Pile

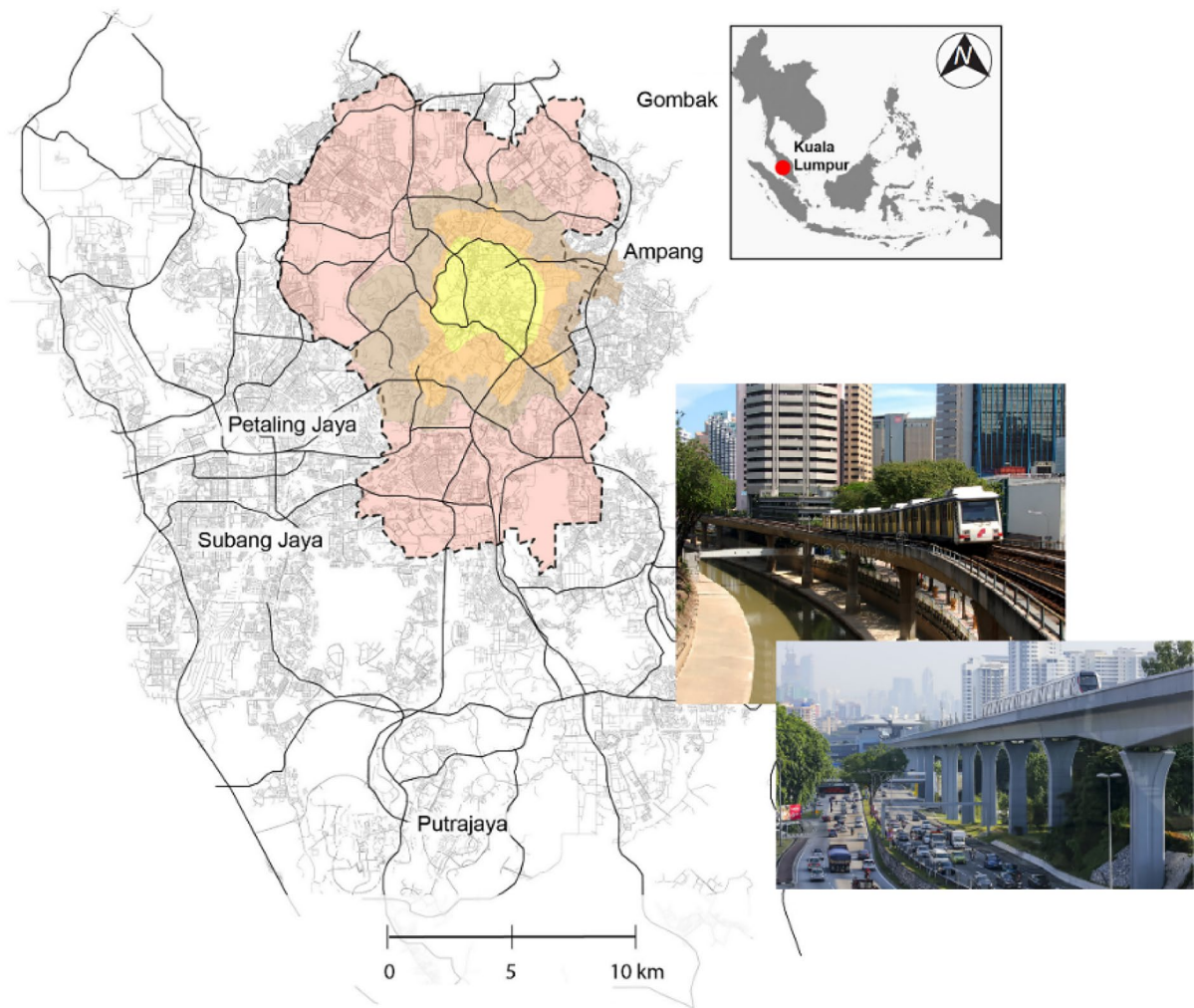


Fig. 1 KVMRT project as study area of research

Dynamic Co manufacture. This was further mentioned earlier that pile diameter and length seem to be parameters affecting the estimated rate of pile settlement. Thus, two variables, the ratio of the length of the pile beneath the soil to that of under rock (L_s/L_r) and the ratio of the total length of the pile to the cross-section pile diameter (L_p/D), were chosen for the analysis of the influence on pile geometry. In addition, due to its effect, UCS is selected as the input model for pile settlement prediction. The N_{SPT} , as input, is also taken to exhibit the status of the soil layers. In addition, the load on the pile has a direct forced effect on the subsidence. Therefore, the ultimate pile load capacity (Q_u) is also taken as an input. Generally, five variables were selected as inputs to

evaluate (PS) pile settlement. Table 1 introduces the target values of PS and inputs of the models accompanied by statistical reports. Figure 2 presents all of the inputs and outputs explained within Fig. 2.

2.2 Support Vector Regression (SVR)

A support vector machine was introduced for classifying and regression issues (Wang 2005). Support vector regression (SVR) was referred to as the regression sort of Support vector machine, which operates a tolerance area (ϵ) for regression outlining. The classifying and regression classes of the SVR approach are served for accomplishing a hyper-plane optimization. Support vector regression

Table 1 The statistical values of the input and output variables

Variable	Symbol	Unit	Max	Min	S. deviation	Average
Standard penetration test	N	–	166.42	2.92	59.08	80.03
Uniaxial compressive strength	UCS	MPa	68.489	25.324	12.442	43.411
Ultimate bearing capacity	Q_u	kN	42,701	12,409	803	2454
Soil length to socket length ratio	L_s/L_r	–	31.714	0.286	6.562	7.063
Pile settlement	SP	mm	20.095	4.494	3.690	10.99
The ratio of total length to diameter	L_p/D	–	31.56	4.33	6.55	15.37

is owned by the supervised learning techniques to discover answers for regression issues via figuring out the following function (Vapnik 2013).

$$min_{w,b} = \frac{1}{2} \|w\|^2 + C \sum_{i=1}^m (\xi_i + \xi_i^*)$$

$$s.t. \left\{ \begin{array}{l} y_i - (w^T x_i + b) \leq \varepsilon + \xi_i \\ (w^T x_i + b) - y_i \leq \varepsilon + \xi_i^* \\ \xi_i, \xi_i^* \geq 0 \end{array} \right. \quad (1)$$

wherein ξ, w, b, ε , and C denote the boundary violation amount, the weight factor, the bias, the deviation rate from the hyperplane, and the regularization parameter in the queue, respectively.

The fitness function contains two parts:

$$\frac{1}{2} \|w\|^2 \quad (2)$$

$$C \sum_{i=1}^m (\xi_i + \xi_i^*) \quad (3)$$

Equation (2) was employed to enhance the area among the samples and hyperplane, and Eq. (3) plays the role of a modifier to preserve the interval among samples with the hyperplane via a unit. Over figuring out the function, the appropriate magnitudes of w and b are gathered, which as targets, seem a hyperplane. The quadratic objective function is used for this research to get better outcomes (Al-Fugara et al. 2020). The main task of the SVR is to solve the optimal values of determinative parameters: ε , σ , and C . For finding them, various optimization algorithms could be employed, in which optimization algorithms, namely Grasshopper Optimization Algorithm and Arithmetic Optimization Algorithm, were coupled with support vector regression to find the parameters of ε , σ ,

and C at optimal levels. Figure 3 tries to show the internal setting of SVR to model the pile settlement based on training data.

2.3 Grasshopper Optimization Algorithm (GOA)

The Grasshoppers are diagnosed as feeder bugs. It has to be cited that grasshoppers are home animals, inflicting critical harm to grasslands and crops (Simpson et al. 1999). They can be free-standing or swarm in the wild. The grasshopper optimization algorithm, which stems from the herbal treatments of grasshoppers, progressed to discover answers to optimize issues (Saremi et al. 2017). Similar to the formerly suggested techniques of optimization rules in the whale, ant-lion, and swarm rules, the first segment is named the exploration segment, and the second is referred to as the mining segment. Rules of the grasshopper optimization algorithm have been changed through locust treatments. The stated steps are considered to discover the meals. Over digging, the nearby motion of the hunt area is chargeable for the actors (Saremi et al. 2017). The conducts for certain degrees of positive parameters with the technique have been explored for bugs’ distant points. Excretion happens at some stage over time intervals (Mafarja et al. 2019). Thus, if the locust’s distance is beyond the range, it suggests that the insect under attention is getting into the consolation zone. Thus, the algorithm of the cumulative move is brought with Eq. (7), wherein x_i shows the position of the i^{th} bug.

$$x_i = r_1 S_i + r_2 G_i + r_3 A_i \quad (4)$$

where, r_1, r_2 and r_3 exhibit the accidental magnitudes between 0 to 1. Also, the variables S_i, A_i , and G_i , denote society’s relationship, the population’s attraction, and gravity, respectively (Cao et al. 2020; Armaghani and Asteris 2021).

Fig. 2 The input and target values and histograms of: **a** L_p/D , **b** L_s/L_r , **c** N_{SPT} , **d** $Q_{u,PS}$, **e** UCS, and **f** PS

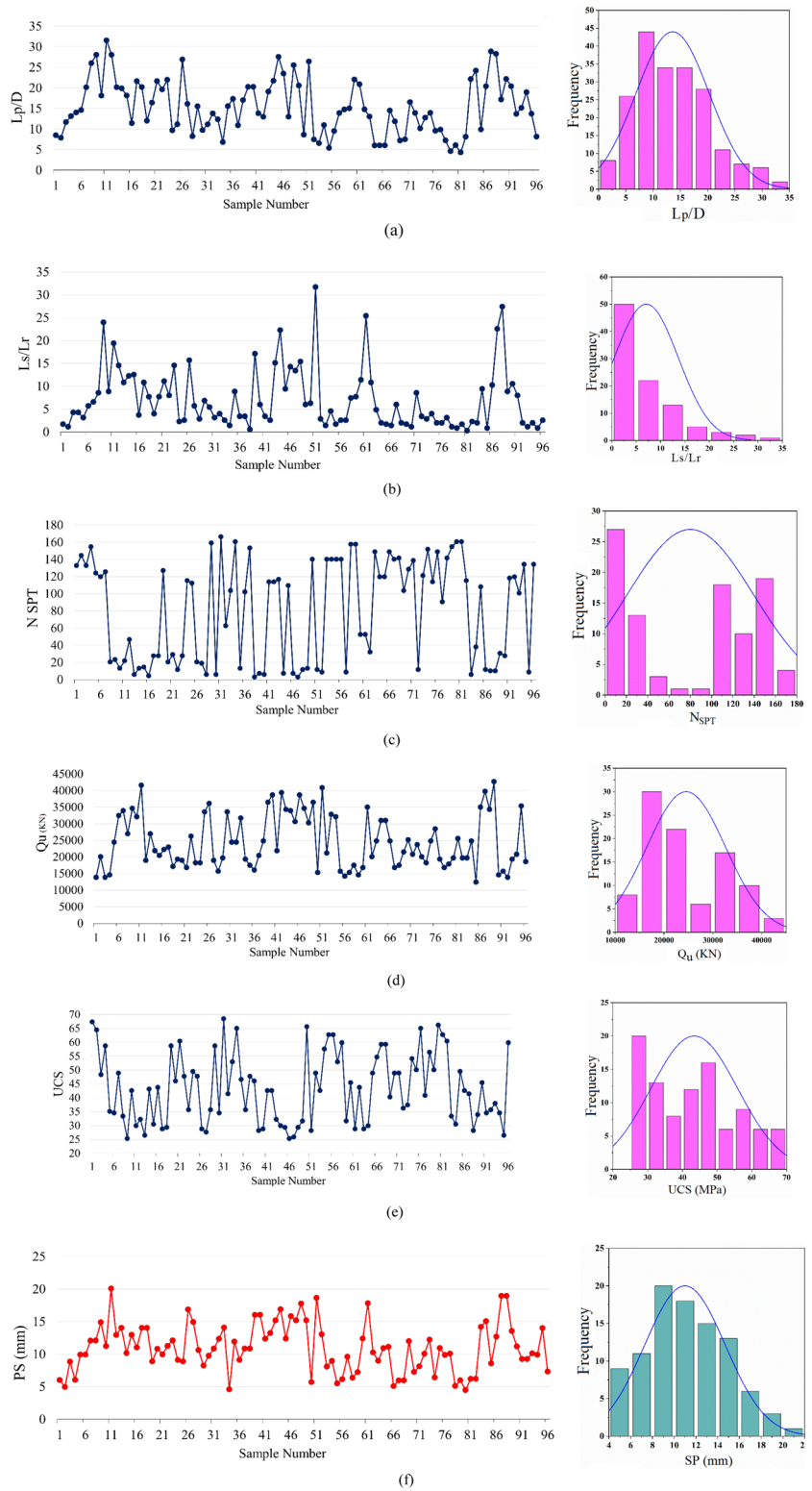


Fig. 3 Pseudo code of support vector regression

Data : Dataset with p^* variables and binary outcome.
Output: Ranked list of variables according to their relevance.

Find the optimal values for the tuning parameters of the SVM model;
 Train the SVM model;
 $p \leftarrow p^*$;
while $p \geq 2$ **do**
 $SVM_p \leftarrow$ SVM with the optimized tuning parameters for the p variables and observations in **Data**;
 $w_p \leftarrow$ calculate weight vector of the SVM_p (w_{p1}, \dots, w_{pp});
 $rank.criteria \leftarrow (w_{p1}^2, \dots, w_{pp}^2)$;
 $min.rank.criteria \leftarrow$ variable with lowest value in $rank.criteria$ vector;
 Remove $min.rank.criteria$ from **Data**;
 $Rank_p \leftarrow min.rank.criteria$;
 $p \leftarrow p - 1$;
end
 $Rank_1 \leftarrow$ variable in **Data** $\notin (Rank_2, \dots, Rank_{p^*})$;
return ($Rank_1, \dots, Rank_{p^*}$)

2.4 Arithmetic Optimization Algorithm (AOA)

The arithmetic optimization algorithm can be considered a candidate-based class with an algebraic concept involving arithmetic operators finding and upgrading the population’s novel location without calculating their derivatives (Abualigah et al. 2021). Arithmetic seems the vital section of present mathematics and looks at one numerical basis algorithm that begins by initializing the candidate solutions created randomly.

$$C = \begin{bmatrix} c_{1,1} & \dots & c_{1,j} \\ \vdots & \ddots & \vdots \\ c_{N,1} & \dots & c_{N,j} \end{bmatrix} \tag{5}$$

The algorithm includes two main parts of exploration and exploitation. The exploration or exploitation search area should be specified and implemented using the math optimizer accelerator function (MOA) to produce the initial candidate.

$$MOA = Min + iter \times \left(\frac{Max - Min}{Max_{iter}} \right) \tag{6}$$

wherein variables of Max and Min represent the maximum and minimum values of MOA. The variable of

$iter$ denotes the current iteration and Max_{iter} Shows the maximum iteration number.

The process of exploration search is conducted by highly distributed magnitudes employing multiplication (M) and division (D) arithmetic operators to the exploration search process. Operators D and M make a high dispersion that cannot assist in reaching the target, but using operators of subtraction (S) and addition (A) arithmetic in the exploitation phase causes reaching the optimum target value.

If $r_1 > MOA$, the exploration phase of the algorithm is in process. The situation in the exploration phase is being updated using Eq. (7), which uses M and D operators.

$$c_{(iter + 1)_{i,j}} = \begin{cases} best(c_j) \div (MOP + \epsilon) \times ((ub - lb) \times \mu + lb)r_2 > 0.5 \\ best(c_j) \div (MOP) \times ((ub - lb) \times \mu + lb) \text{ otherwise} \end{cases} \tag{7}$$

wherein, $best(c_j)$ denotes the best location, ub , and lb are the upper and lower boundary of the area for search. ϵ denotes a small value, and μ adjusts the parameter for controlling the search and is set to 0.499 for the model. MOP is specified as math optimization probability and is calculated with Eq. (8).

$$MOP(iter) = 1 - \frac{iter^{1/\alpha}}{Max_{iter}^{1/\alpha}} \quad (8)$$

In which α denotes the exploitation accuracy sensitivity over the iterations and is considered 5.

Notably, when $r_1 < MOA$, the exploitation stage happens in this phase when operators of S and A are employed for a deep search of the dense area. This deep searching is modeled with Eq. (9).

$$c(iter+1)_{i,j} = \begin{cases} best(c_j) - (MOP) \times ((ub - lb) \times \mu + lb)r_3 > 0.5 \\ best(c_j) + (MOP) \times ((ub - lb) \times \mu + lb) \text{ otherwise} \end{cases} \quad (9)$$

Figure 4 shows the performance of the AOA optimizer in finding hyperparameters' rate at an optimal level for SVR.

The conceptual relation in a combination of optimizers with Support Vector Regression is presented in Figure 5.

2.5 Performance Evaluation via Special Criteria

Table 2 represents the indices that survey the hybrid SVR frameworks' performance.

Fig. 4 Pseudo code of archimedes optimization algorithm (AOA)

```

procedure AOA (population size  $N$ , maximum iterations  $t_{max}$ ,  $C1$ ,  $C$ ,  $C3$ ,  $C4$ )
  Initialize objects population with random positions, densities and volumes
  Evaluate initial population and select the one with the best fitness value
  Set iteration counter  $t = 1$ 
  while  $t < t_{max}$  do
    for each object  $i$  do
      Update density and volume of each object
      Update transfer and density decreasing factors  $T$ ,  $F$ ,  $d$ 
      if  $T \cdot F < 0.5$  then  $\rightarrow$  Exploration phase
        Update acceleration and normalize acceleration
        Update position
      else  $\rightarrow$  Exploitation phase
        Update acceleration and normalize acceleration
        Update direction flag  $F$ 
        Update position
      end if
    end for
    Evaluation each object and select the one with the best fitness value
    Set  $t=t+1$ 
  
```

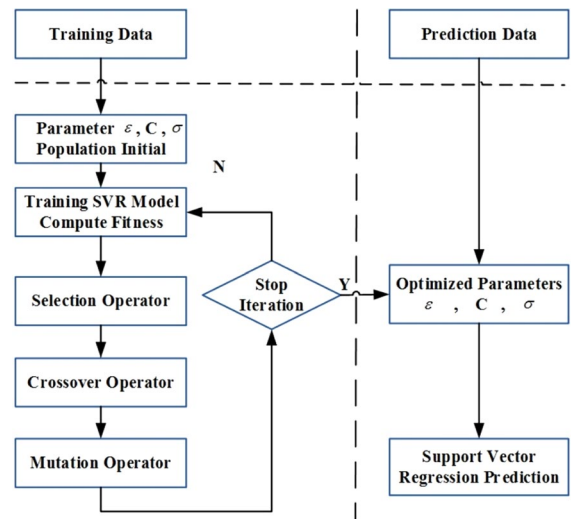


Fig. 5 Conceptual relation in a combination of support vector regression with optimizers

3 Result and Discussion

The hybrid SVR machine learning technique outcomes, SVR-AOA and SVR-GOA, to forecast the rate of pile settlement were produced, shown in the present part. The complexity and cost of modeling accompanied

Table 2 The evaluation indices used for the models’ examination

Index	Symbolism	Equation	status
Variance account factor	<i>OBJ</i>	$\left(\frac{n_{train}-n_{test}}{n_{train}+n_{test}}\right) \frac{RMSE_{train}+MAE_{test}}{R_{train}^2+1} + \left(\frac{2n_{train}}{n_{train}+n_{test}}\right) \frac{RMSE_{test}-MAE_{test}}{R_{test}^2+1}$	Low = desirable
Mean absolute error	<i>MAE</i>	$\frac{1}{N} \sum_{n=1}^N p_n - t_n $	Low = desirable
Pearson’s correlation coefficient	<i>R</i>	$\frac{\sum_{n=1}^N (t_n - \bar{t})(p_n - \bar{p})}{\sqrt{[\sum_{n=1}^N (t_n - \bar{t})^2][\sum_{n=1}^N (p_n - \bar{p})^2]}}$	High = desirable
Root mean squared error	<i>RMSE</i>	$\sqrt{\frac{1}{N} \sum_{n=1}^N (p_n - t_n)^2}$	Low = desirable
Variance account factor	<i>VAF</i>	$\left(1 - \frac{var(t_n - y_n)}{var(t_n)}\right) * 100$	High = desirable

Wherein, p_N shows the predicted magnitude; t_n is n^{th} target value; \bar{t} shows the average of measured data; \bar{p} is the averaged target values that are predicted. Further, the n_{train} and n_{test} exhibit the data number in the train and test steps

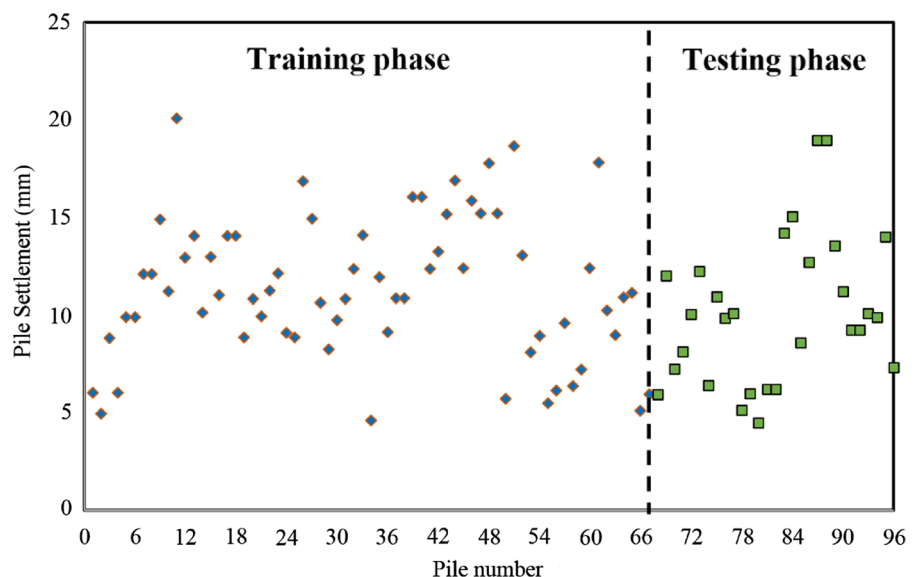
by increasing appraising accuracy are considered, and these factors must be smoothed via optimizers utilized in this research. A MATLAB environment implemented the simulations. The scattered plot of the measured pile settlement ranges within the KVMRT project has been shown in Fig. 6, wherein 70 and 30 percent of measured data have been considered for, alternatively, training and testing phases. The suitable magnitudes of ϵ , σ , and C of SVR for the data set lead to maximum determination coefficient and RMSE at minimum for SVR-AOA have been calculated as 0.6 and 0.554, respectively. Moreover, these values for SVR-GOA were 0.65 and 0.597, alternatively.

The SVR-AOA modeling to predict the subsidence rate of each pile was done, and the results are shown

in Fig. 7. Overall, the prediction process has been done in a desirable way defined by R , and $RMSE$ acquired as 0.99 and 0.55 mm. Further, the best trend line shows the appropriate correctness of modeling placed adjacent to the dashed bisector line with the overestimation for settlement rates below 12 mm and underestimation for higher than this magnitude. The slope of the best-fit trend line with around 0.9 also implies a suitable simulation with the model coupled with the AOA optimizer.

Similar to the SVR-AOA model, SVR-GOA results are brought up via Fig. 8. At first look, the prediction process has been done in a desirable way that is definite by R and $RMSE$ calculated as 0.99 and 0.59 mm. Further, the best trend line shows the appropriate correctness of modeling placed adjacent to the dashed

Fig. 6 In-situ pile settlement data within the KVMRT project



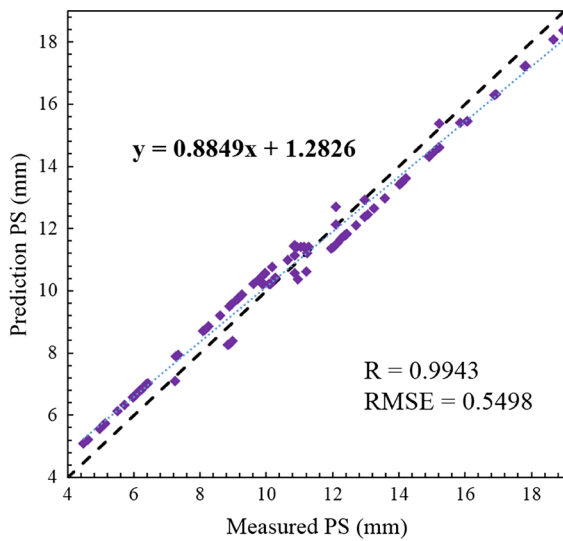


Fig. 7 The SVR-AOA plot of measurement and predicted settlement rates

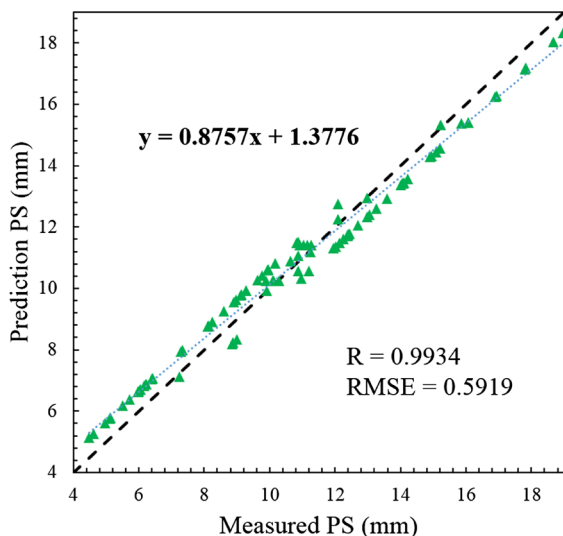


Fig. 8 The SVR-GOA plot of measurement and predicted settlement rates

bisector line with the overestimation for settlement rates below 12 mm and underestimation for higher than this magnitude. The slope of the best-fit trend line with around 0.9 also implies suitable simulation with the model coupled with GOA optimizer.

As depicted in Figs. 7 and 8, by comparing both of them, SVR-AOA demonstrated higher appropriate

magnitudes for RMSE and R than SVR-GOA of 0.10% and 7.66%, alternatively. AOA could fulfil well for optimizing modeling performance because the points scattered around the best-fit line seem adjacent compared with those in GOA. Especially the piles involving large numbers have been modeled close to the actual measurement with minimal error. This can be accounted for by applying 70% of the data to train in the neural network.

In continuous, Table 3 shows modeling functionality for every hybrid framework and the usage of the VAF, R, MAE, OBJ, and RMSE indices (within Table 2). Each level of the train and test stage presents the same result. In the train section, the optimization set of AOA has fulfilled higher with the aid of using evaluating indices as acceptable compared to the consequences of GOA. The index of MAE has been given the maximum discrepancy with approximately 7.10% for SVR-AOA. However, the results of VAF and R-value indexes have not attracted interest with moderate distinction by the same performance. Identically, all indices of R, OBJ, MAE, VAF, and RMSE associated with the test stage for SVR-AOA had been located an acceptable degree in assessment with SVR-GOA with the aid of using the RMSE as acquired 7.62%. Moreover, the OBJ index, including the R, RMSE, and MAE in each level of train and test, offers a higher accuracy of modeling process for SVR-AOA that serves with 0.54 mm mistake in modeling pile settlement.

For a clear sight of the correctness of modeling, Fig. 9 attempts to show modeling errors for each pile rather than measured target values. They use Fig. 9 in cases where the measurements and the model line do not coincide. Many of the modeling parts are correctly done, as seen in both sections of the test and train phases. This chart has shown the extent to which the deviations between the models and the actual measurements are significant.

The SVR-AOA (a) model was modeled closest to the in-situ measurements in the diagram. However, the gap between modeling and measurement for piles nine and ten becomes larger than for other parts. Similarly, for SVR-GOA (b), this story runs indeed that bypassing the dashed line as the border of test and train phases, modeling accuracy has been enhanced to a better rate.

Figure 10 shows the best sight for modeling performance analysis. The scheme in question refers

Table 3 Evaluation of models' performance

			SVR-GOA	SVR-AOA	Difference (%)
Criteria to assess	Train stage	<i>R</i>	0.992	0.993	0.11%
		<i>RMSE</i>	0.59	0.548	7.68%
		<i>MAE</i>	0.559	0.522	7.10%
		<i>VAF</i>	99.73	99.789	0.06%
	Test stage	<i>R</i>	0.995	0.996	0.07%
		<i>RMSE</i>	0.596	0.554	7.62%
		<i>MAE</i>	0.564	0.532	5.88%
		<i>VAF</i>	99.724	99.828	0.10%
<i>OBJ</i>			0.541	0.586	8.26%

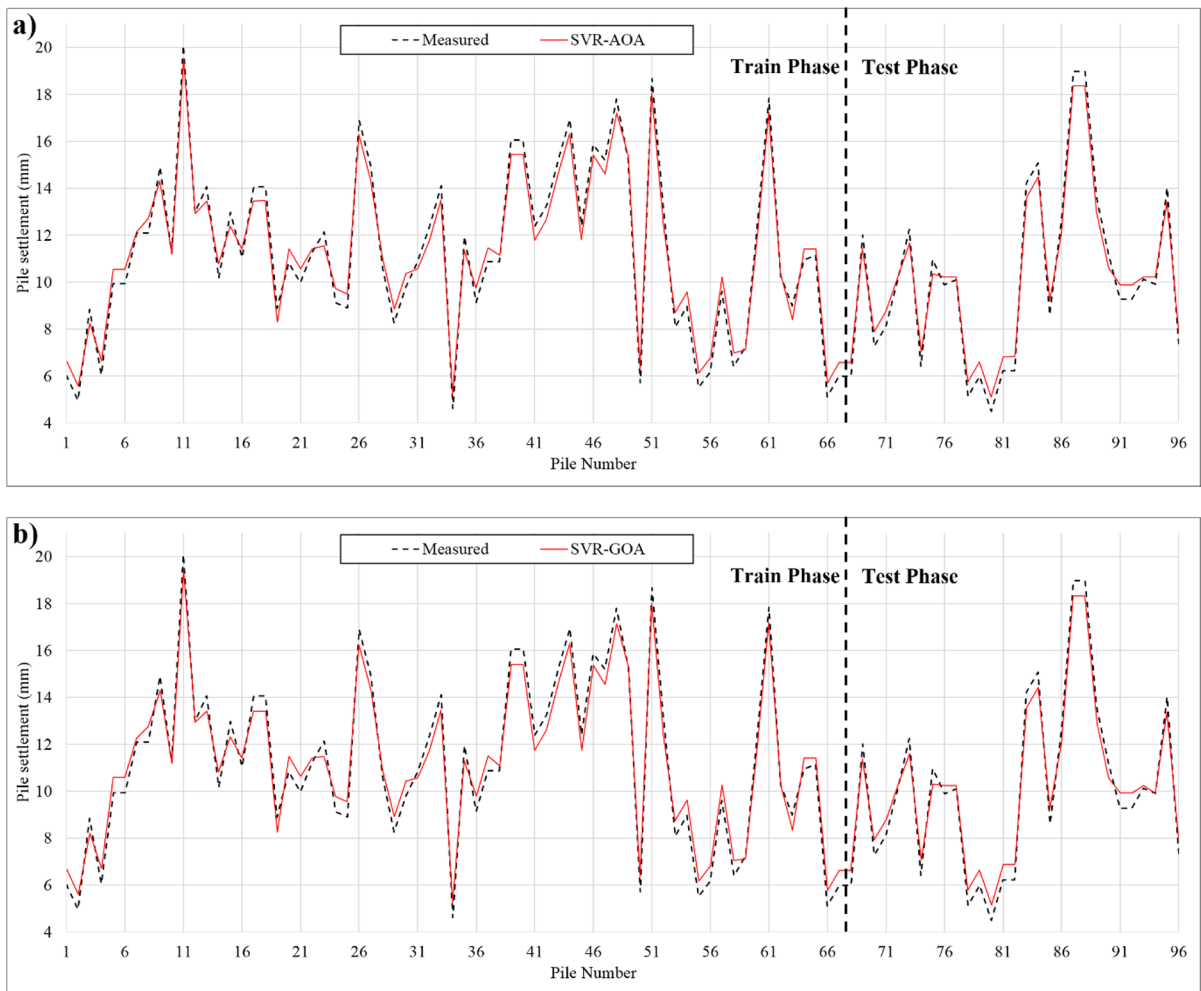


Fig. 9 Modeled PS and measured data for each pile in **a** SVR-AOA and **b** SVR-GOA

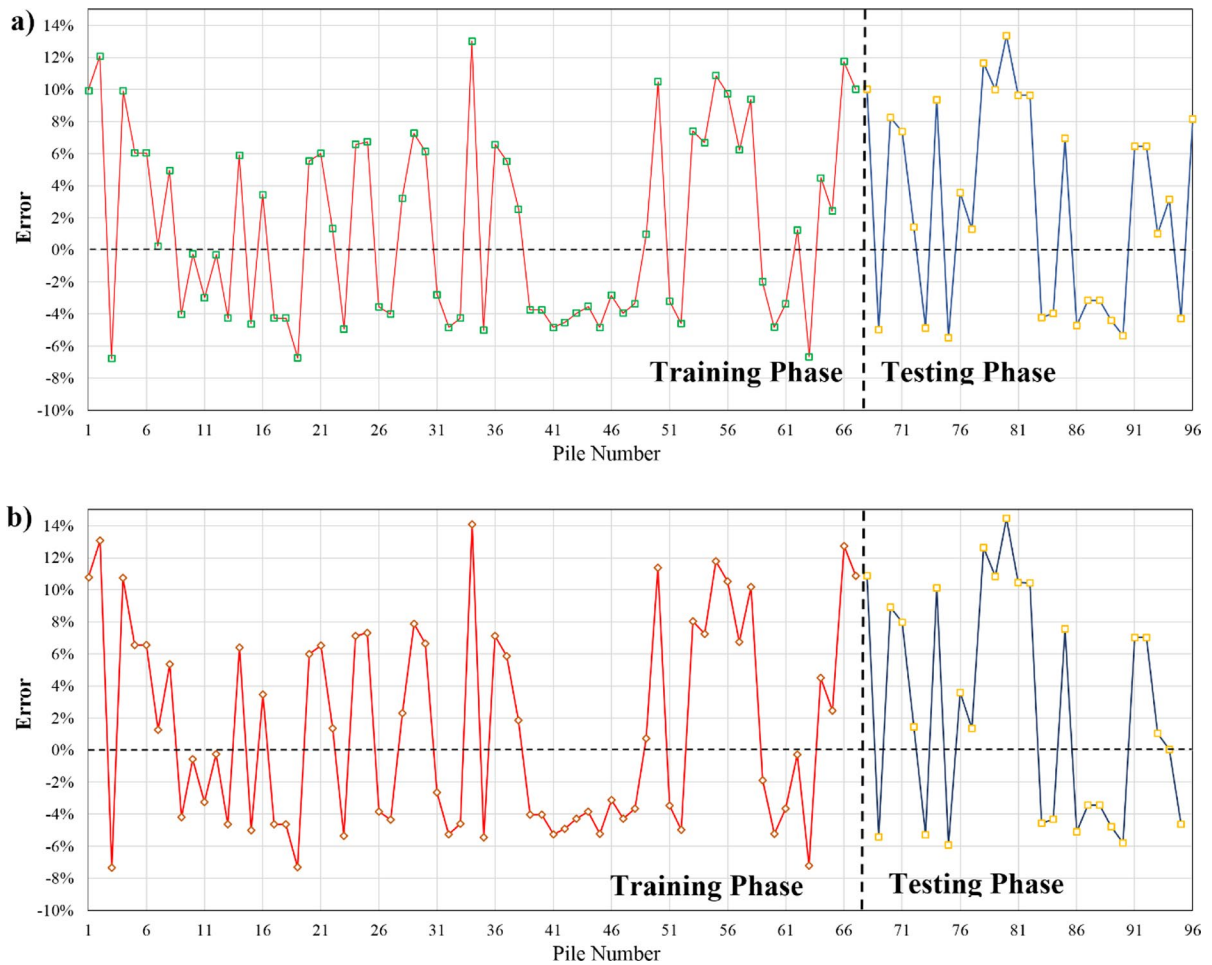


Fig. 10 The modeling error in **a** SVR-AOA and **b** SVR-GOA

to the mistakes in achieving the target for the piles modeled in terms of measured values of positive (overestimated) and negative (underestimated). Thus, according to Fig. 10, diagram (a), SVR-AOA shows that the error in the simulation of pile motion during the training period is close to a maximum of 14%. However, during the testing phase, the error rate increased slightly but was too close to a 14% error line. Moreover, SVR-GOA (b) has completed its defining task of modeling pile settlement with a larger error than SVR-AOA. Actually, for the training period, the error of SVR-GOA exceeds 14%. This border has exceeded the maximum error of the previous step in the test step.

Next, the distribution of errors and the normal distribution of modeling errors for both hybrid

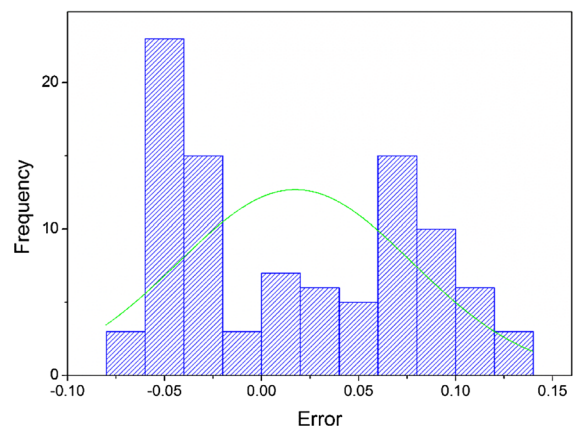


Fig. 11 Error distribution in the SVR-AOA model

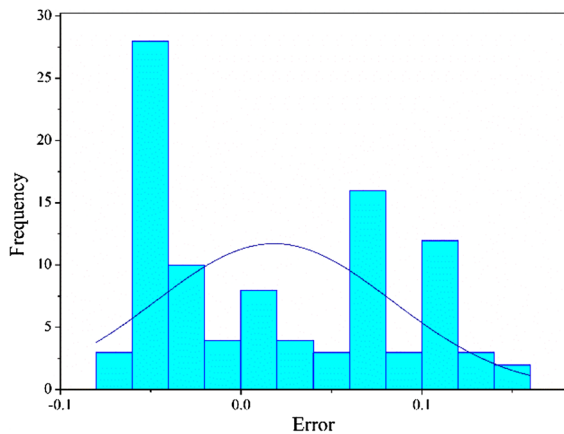


Fig. 12 Error distribution in the SVR-AOA model

models will be exhibited. Figure 11 shows the error distribution in frequency and the standard error distribution curve.

Concentrating errors not around the center of zero magnitudes on the horizontal error axis has led to the flattened shape of the standard distribution error curve. Maximum frequency for the error as the high histogram is found for around 25 with about -0.05. Also, Fig. 12 shows a similar exhibition for the SVR-GOA framework. For this model, identically, the standard curve has been shaped flattened so that this matter stems from error concentration, not in the center of zero point. Compared to the SVR-AOA, the tall histogram of error around -0.05 has 26 frequencies, the same pattern in the modeling process.

Although SVR via the AOA performed better in modeling the pile settlement with appropriate results, the SVR-GOA has had the same pattern error distribution. Based on the results, Arithmetic Optimization Algorithm was more mighty than Grasshopper Optimization Algorithm with the sign of accurate calculation of SVR parameters. The differences in correlation and error rates for the two hybrid models are derived from various AOA and GOA internal settings. However, both optimizers regulated the SVR model to generate PS rates with an average correlation of 0.99.

4 Conclusion

The goal of the current study is to simulate the pile settlement using the Support Vector Regression (SVR) neural network, in which two optimization algorithms, as Arithmetic Optimization Algorithm (AOA) and Grasshopper Optimization Algorithm (GOA), have been operated to predict the better regression to calculate the pile settlement rates that would reduce the cost and complexity of network computations. For using coupled frameworks of SVR-AOA and SVR-GOA, the pile tests, their measurements, and earth properties were obtained for the Klang Valley Mass Rapid Transit (KVMRT) transportation project in Kuala Lumpur city.

Each framework developed had the desirable capability to estimate the dependent pile settlement variable, where the R -value of the training step was obtained on average 0.993 and 0.996 in the testing step for both SVR-AOA and SVR-GOA. Alternatively, that shows a 0.3 percent difference.

Overall, SVR-AOA could be given the allowable results via the indices for evaluating each method. SVR-AOA framework, statistically, with the appropriate numbers of R , RMSE, MAE, and VAF at 0.994, 0.55, 0.525, and 99.806 had suitable performance compared to SVR-GOA with mentioned criteria of 0.993, 0.592, 0.561, and 99.734, respectively, in which the higher difference is for RMSE by 7.66%. In the training step, including 70 percent of data, SVR-AOA could get 0.993 for R 0.11% is higher than SVR-GOA modeling results. Also, RMSE, MAE, and VAF of SVR-AOA in the training step were calculated at 0.548, 0.522, and 99.789, which were better rates by 7.68%, 7.10%, respectively, and 0.06% improvement. The comprehensive OBJ index includes the R , RMSE, and MAE indexes of errors and correlation indices. SVR-GOA and SVR-AOA obtained values of 0.541 and 0.586 mm, respectively, with a difference of 8.26%. Generally, hybrid models and artificial intelligent-based models can increase the accuracy of estimating pile settlement to substitute actual practical experiments and reduce the time and cost.

Author Contributions Authors are equally contributed in all parts of the present work.

Funding This work was supported by the Key Project of University-level Teaching and Research Projects (Research on the Teaching Reform of Civil Engineering Graduation

Design in application-oriented Universities Under the Background of New Engineering, No. wxxy2021032), Provincial Ideological and Political Demonstration Course (Construction Engineering Economy, No.2021kcszsfkc441), Key Project of Natural Science Research of Education Department of Anhui Province (Study on fire resistance of concrete-filled steel tube core column-reinforced concrete beam joint, No.KJ2018A0412), University-level Ideological and Political Demonstration Course (Theoretical Mechanics Architecture major, No. wxxy2021142), Key Project of Provincial-level Teaching and Research Projects (Research on Civil Mechanics course based on College students Mechanics competition, No. 2020jyxm2144), Key Project of Natural Science Research of Education Department of Anhui Province (Study on structural performance and engineering application of autoclaved aerated concrete slab, No. KJ2021A0948).

Data Availability The applied data in the present work is available at the reasonable request of the authors.

Declarations

Conflict of interest The authors declare no competing interests.

References

- Abualigah L, Diabat A, Mirjalili S et al (2021) The arithmetic optimization algorithm. *Comput Methods Appl Mech Eng* 376:113609. <https://doi.org/10.1016/j.cma.2020.113609>
- Acosta SM, Amoroso AL, Sant Anna AMO, Canciglieri Junior O (2021) Relevance vector machine with tuning based on self-adaptive differential evolution approach for predictive modelling of a chemical process. *Appl Math Model* 95:125–142. <https://doi.org/10.1016/j.apm.2021.01.057>
- Acosta SM, Oliveira RMA, Sant'Anna AMO (2023) Machine learning algorithms applied to intelligent tyre manufacturing. *Int J Comput Integr Manuf.* <https://doi.org/10.1080/0951192X.2023.2177734>
- Alemdag S, Gurocak Z, Cevik A et al (2016) Modeling deformation modulus of a stratified sedimentary rock mass using neural network, fuzzy inference and genetic programming. *Eng Geol* 203:70–82
- Al-Fugara A, Ahmadlou M, Al-Shabeeb AR et al (2020) Spatial mapping of groundwater springs potentiality using grid search-based and genetic algorithm-based support vector regression. *Geocarto Int.* <https://doi.org/10.1080/10106049.2020.1716396>
- Alilou VK, Yaghmaee F (2015) Application of GRNN neural network in non-texture image inpainting and restoration. *Pattern Recognit Lett* 62:24–31
- Alkroosh I, Nikraz H (2011) Correlation of pile axial capacity and CPT data using gene expression programming. *Geotech Geol Eng* 29:725–748
- Armaghani DJ, Asteris PG (2021) A comparative study of ANN and ANFIS models for the prediction of cement-based mortar materials compressive strength. *Neural Comput Appl* 33:4501–4532
- Bendu H, Deepak B, Murugan S (2016) Application of GRNN for the prediction of performance and exhaust emissions in HCCI engine using ethanol. *Energy Convers Manag* 122:165–173
- Benemaran RS, Esmaili-Falak M (2020) Optimization of cost and mechanical properties of concrete with admixtures using MARS and PSO. *Comput Concr.* <https://doi.org/10.12989/cac.2020.26.4.309>
- Cao Y, Babanezhad M, Rezakazemi M, Shirazian S (2020) Prediction of fluid pattern in a shear flow on intelligent neural nodes using ANFIS and LBM. *Neural Comput Appl* 32:13313–13321
- Che WF, Lok TMH, Tam SC, Novais-Ferreira H (2003) Axial capacity prediction for driven piles at Macao using artificial neural network
- Chen H, Li X, Wu Y et al (2022) Compressive strength prediction of high-strength concrete using long short-term memory and machine learning algorithms. *Buildings* 12:302
- Dindarloo SR (2015) Prediction of blast-induced ground vibrations via genetic programming. *Int J Min Sci Technol* 25:1011–1015
- Gao W, Han J (2020) Prediction of destroyed floor depth based on principal component analysis (PCA)-genetic algorithm (GA)-support vector regression (SVR). *Geotech Geol Eng* 38:3481–3491. <https://doi.org/10.1007/s10706-020-01227-3>
- Goh ATC (1996) Pile driving records reanalyzed using neural networks. *J Geotech Eng* 122:492–495. [https://doi.org/10.1061/\(ASCE\)0733-9410\(1996\)122:6\(492\)](https://doi.org/10.1061/(ASCE)0733-9410(1996)122:6(492))
- Hanna AM, Morcous G, Helmy M (2004) Efficiency of pile groups installed in cohesionless soil using artificial neural networks. *Can Geotech J* 41:1241–1249
- Hatheway AW (2009) The complete ISRM suggested methods for rock characterization, testing and monitoring; 1974–2006. *Environ Eng Sci* 15:47–48
- Kumar M, Samui P (2020) Reliability analysis of settlement of pile group in clay using LSSVM, GMDH, GPR. *Geotech Geol Eng* 38:6717–6730
- Le T-T, Le MV (2021) Development of user-friendly kernel-based Gaussian process regression model for prediction of load-bearing capacity of square concrete-filled steel tubular members. *Mater Struct* 54:1–24
- Lee I-M, Lee J-H (1996) Prediction of pile bearing capacity using artificial neural networks. *Comput Geotech* 18:189–200
- Liu H, Li TJ, Zhang YF (1997) The application of artificial neural networks in estimating the pile bearing capacity
- Ma H, Peng C (2023) Analysis and application of ultimate bearing capacity of squeezed branch pile. *Geotech Geol Eng.* <https://doi.org/10.1007/s10706-023-02461-1>
- Ma G, Chao Z, He K (2021) Predictive models for permeability of cracked rock masses based on support vector machine techniques. *Geotech Geol Eng* 39:1023–1031. <https://doi.org/10.1007/s10706-020-01542-9>
- Mafarja M, Aljarah I, Faris H et al (2019) Binary grasshopper optimisation algorithm approaches for feature selection problems. *Expert Syst Appl* 117:267–286
- Masoumi F, Najjar-Ghabel S, Safarzadeh A, Sadaghat B (2020) Automatic calibration of the groundwater simulation model with high parameter dimensionality using

- sequential uncertainty fitting approach. *Water Supply* 20:3487–3501. <https://doi.org/10.2166/ws.2020.241>
- Mishra A, Sawant VA, Deshmukh VB (2019) Prediction of pile capacity of socketed piles using different approaches. *Geotech Geol Eng* 37:5219–5230
- Mollahasani A, Alavi AH, Gandomi AH (2011) Empirical modeling of plate load test moduli of soil via gene expression programming. *Comput Geotech* 38:281–286
- Momeni E, Dowlatshahi MB, Omidinasab F et al (2020) Gaussian process regression technique to estimate the pile bearing capacity. *Arab J Sci Eng* 45:8255–8267
- Moodi Y, Ghasemi M, Mousavi SR (2022) Estimating the compressive strength of rectangular fiber reinforced polymer-confined columns using multilayer perceptron, radial basis function, and support vector regression methods. *J Reinf Plast Compos* 41:130–146
- Ozbek A, Unsal M, Dikec A (2013) Estimating uniaxial compressive strength of rocks using genetic expression programming. *J Rock Mech Geotech Eng* 5:325–329
- Pal M, Deswal S (2010) Modelling pile capacity using Gaussian process regression. *Comput Geotech* 37:942–947
- Poulos HG (1989) Pile behaviour—theory and application. *Geotechnique* 39:365–415
- Poulos HG (2006) Pile group settlement estimation—Research to practice. *Found Anal Des Innov Methods*. [https://doi.org/10.1061/40865\(197\)1](https://doi.org/10.1061/40865(197)1)
- Randolph MF (2003) Science and empiricism in pile foundation design. *Géotechnique* 53:847–875
- Saggu R (2022) Cyclic pile-soil interaction effects on load-displacement behavior of thermal pile groups in sand. *Geotech Geol Eng* 40:647–661
- Samui P (2019) Determination of friction capacity of driven pile in clay using Gaussian process regression (GPR), and minimax probability machine regression (MPMR). *Geotech Geol Eng* 37:4643–4647
- Saremi S, Mirjalili S, Lewis A (2017) Grasshopper optimisation algorithm: theory and application. *Adv Eng Softw* 105:30–47
- Shahin MA, Maier HR, Jaksa MB (2002) Predicting settlement of shallow foundations using neural networks. *J Geotech Geoenvironmental Eng* 128:785–793
- Shanbeh M, Najafzadeh D, Ravandi SAH (2012) Predicting pull-out force of loop pile of woven terry fabrics using artificial neural network algorithm. *Ind Textila* 63:37–41
- Simpson SJ, McCaffery AR, Hägele BF (1999) A behavioural analysis of phase change in the desert locust. *Biol Rev* 74:461–480
- Soleimanbeigi A, Hatf N (2006) Prediction of settlement of shallow foundations on reinforced soils using neural networks. *Geosynth Int* 13:161–170
- Stewart DP, Jewell RJ, Randolph MF (1994) Design of piled bridge abutments on soft clay for loading from lateral soil movements. *Geotechnique* 44:277–296
- Teh CI, Wong KS, Goh ATC, Jaritngam S (1997) Prediction of pile capacity using neural networks. *J Comput Civ Eng* 11:129–138
- Teodorescu L, Sherwood D (2008) High energy physics event selection with gene expression programming. *Comput Phys Commun* 178:409–419
- Vapnik V (2013) *The nature of statistical learning theory*. Springer science & business media, Berlin
- Wang L (2005) *Support vector machines: theory and applications*. Springer Science & Business Media, Berlin
- Wu J, Long J, Liu M (2015) Evolving RBF neural networks for rainfall prediction using hybrid particle swarm optimization and genetic algorithm. *Neurocomputing* 148:136–142
- Xu L, Qian F, Li Y et al (2016) Resource allocation based on quantum particle swarm optimization and RBF neural network for overlay cognitive OFDM System. *Neurocomputing* 173:1250–1256
- Zendehboudi A, Tatar A (2017) Utilization of the RBF network to model the nucleate pool boiling heat transfer properties of refrigerant-oil mixtures with nanoparticles. *J Mol Liq* 247:304–312
- Zhang WG, Goh ATC (2013) Multivariate adaptive regression splines for analysis of geotechnical engineering systems. *Comput Geotech* 48:82–95
- Zhang Y, Hu X, Tannant DD et al (2018a) Field monitoring and deformation characteristics of a landslide with piles in the three Gorges reservoir area. *Landslides* 15:581–592
- Zhang Y, Richardson DC, Barnouin OS et al (2018b) Rotational failure of rubble-pile bodies: influences of shear and cohesive strengths. *Astrophys J* 857:15

Publisher's Note Springer Nature remains neutral with regard to jurisdictional claims in published maps and institutional affiliations.

Springer Nature or its licensor (e.g. a society or other partner) holds exclusive rights to this article under a publishing agreement with the author(s) or other rightsholder(s); author self-archiving of the accepted manuscript version of this article is solely governed by the terms of such publishing agreement and applicable law.